Th-AM-J5

STRUCTURAL DETAILS OF A CALCIUM INDUCED MOLECULAR SWITCH: COMPARISON OF THE HIGH RESOLUTION, X-RAY CRYSTALLOGRAPHIC STRUCTURES OF THE CALCIUM-FILLED AND CALCIUM-FREE FORMS OF THE N-TERMINAL REGULATORY DOMAIN OF TROPONIN C. ((N.C.J. Strynadka, M. Chemaia, M. Li, L.B. Smillie and M.N.G. James)) The MRC Group in Protein Structure and Function, Department of Biochemistry, University of Alberta, Edmonton, Alberta, Canada, T6G 2H7

The binding of calcium ions to the N-terminal regulatory domain of troponin C elicits a conformational change which constitutes the major intracellular signal for the initiation of muscle contraction (1). Due to the low pH of the crystallization media, the original x-ray crystallographic structure of troponin C (2,3) had the N-terminal domain in the calcium-free state. Recently the N-terminal domain of chicken skeletal TnC has been cloned, expressed (4) and crystallized at pH 7.5. The x-ray crystallographic structure of the calcium loaded N-terminal domain has been solved to high resolution (1.6 Ang.). A detailed comparison of the molecular changes in the calcium free and calcium filled state of the domain will be discussed.

1) Zot, A.S., and Potter, J.D. 1987 Ann. Rev. Biophys. Biophys. Chem. 16:535-559
2) Herzberg, O. and James, M.N.G. 1985 Nature 313:653-659
3) Sundarlingam, M. *et al.* 1985 Science 227:945-948
4) Li, M.X., Chandra, M., Pearlstone, J., Racher, K.I., Trigo-Gonzalez, G., Borgford, T., Kay, C.M., and Smillie, L.B. 1994 Biochemistry 33 917-925

Th-AM-J6

CALMODULIN HAS AN EXTENDED CONFORMATION WHEN COMPLEXED WITH SMOOTH MUSCLE CALDESMON. ((Y. Mabuchi, C.-L.A. Wang & Z, Grabarek)) Muscle Research Group, Boston Biomedical Research Institue, Boston, MA 02114.

CaM34/110 is a mutant of human liver calmodulin with Cys residues substituted for Thr34 and Thr110. The global conformation of CaM34/110 can be monitored by energy transfer between a donor (AEDANS, N-iodoacetyl-N'-(5-sulfo-1-naphthyl)ethylenediamine) and an acceptor (DAB, 4-dimethyl -aminophenylazophenyl-4'-maleimide) attached to the Cys residues. Upon complex formation between CaM34/110-AEDANS/DAB and caldesmon (CaD) there is an increase in the AEDANS fluorescence intensity indicating an increase in the average distance between the probes. The C-terminal 22 kDa recombinant fragment of CaD (residues 579-756) is also capable of inducing a similar increase in the fluorescence of CaM34/110-AEDANS/DAB, however the three short synthetic peptides of CaD corresponding to the putative CaM binding sites: GS17C (651-667), MG56C (658-713) and VG29C (685-713) are ineffective in this respect, although they bind to CaM34/110. These results indicate that the conformation of CaM in the complex with CaD is extended, similar to that reported for free CaM (Babu et al. Nature 315,37,1985) and unlike that reported for the CaM-M13 complex (Ikura et al. Science 256,632,1992; Meador et al. Science 257,1251,1992). It appears that some stabilization of the CaM-binding regions of CaD by other parts of the C-terminal domain of CaD is necessary for their ability to induce the correct conformation in CaM. Alternatively, there may be another, yet unidentified, CaM-binding segment in the C-terminal domain of CaD which accounts for the difference in the properties of the 22 kDa fragment and the shorter peptides. (Supported by NIH, AR-41156, AR-41637)

Th-AM-J7

CALDESMON CONTROLS ACTOMYOSIN ATPASE AND FILAMENT MOTILITY BY SWITCHING ACTIN-TROPOMYOSIN FROM THE 'ON' TO THE 'OFF' STATE ((S.B. Marston and I.D.C. Fraser))
Dept. Cardiac Medicine, NHLI, Dovehouse St., LONDON SW3 6LY, UK

We compared the effect of inhibitory concentrations of caldesmon, caldesmon fragment H9 (C-terminal 69 amino acids of human caldesmon) and troponin upon the interaction of the strongly binding species S-1.AMP.PNP and NEM-S-1 with actin-smooth muscle tropomyosin (Atm) at 0.03M ionic strength. At low concentrations of S1.AMP.PNP all the inhibitors reduced afinity for ATm >20 fold and the binding curve was highly cooperative . 0.1 NEM-S-1/actin potentiated Atm activation of myosin MgATPase 6-fold. Caldesmon inhibited the ATPase in the presence and absence of NEM-S-1. NEM-S-1 reactivated Atm ATPase which had been inhibited by troponin, caldesmon or H9. Thus in solution caldesmon and troponin inhibition is associated with inhibiting strong crossbridge binding by switching the actin-tropomyosin 'on'/'off' equilibrium towards the 'off' state.
We also studied caldesmon control of Atm in an *in vitro* motility assay. Actin-smooth muscle tropomyosin moving over immobilised skeletal muscle HMM was measured at I=0.08M, 28°C in 0.5% methylcellulose. 40nM tm increased the velocity of actin filament movement from 3.46 to 4.40 μm/ sec, confirming that the smooth muscle Atm complex is predominantly in the 'on' state. Addition of caldesmon did not reduce filament velocity, however as concentration increased more and more actin filaments stopped moving. Most of the filaments stopped moving at caldesmon concentrations (25nM) which had little effect upon the number of actin filaments associated with HMM. Thus, as in solution, caldesmon inhibition involves mainly strongly bound actin-myosin complexes and is highly cooperative; a whole actin filament is switched on or off as a unit.

Th-AM-J8

CALDESMON, CALPONIN, AND TROPOMYOSIN REGULATE IN VITRO MOTILITY AND ISOMETRIC FORCE PRODUCTION BY DEPHOSPHORYLATED CROSS BRIDGES. ((J.R. Haeberle)) Dept.Molecular Physiology and Biophysics, The University of Vermont, Burlington, VT, 05405

We previously reported that the activation of isometric force by myosin light chain phosphorylation was highly cooperative for regulated thin filaments reconstituted with calponin and tropomyosin. We proposed that dephosphorylated cross bridges were being activated by "turned-on" thin filaments, and that calponin promoted the turning-on of thin filaments by slowing the dissociation rate of the high-affinity phosphorylated cross bridges. In the present study, caldesmon is shown to completely inhibit the calponin-tropomyosin-dependent recruitment of dephosphorylated cross bridges at concentrations that have no effect on force production by phosphorylated cross bridges. Isometric force production was measured using an in vitro motility assay and a simple method for measuring isometric force using NEM-modified myosin to mechanically load thin filaments. Relative changes in isometric force were measured as the minimum molar ratio of NEM-modified/unmodified myosin that halted filament motion. Force was measured as a function of the % thiophosphorylated myosin, for reconstituted thin filaments containing tropomyosin, caldesmon, and calponin. Reconstituted filaments containing saturating tropomyosin and 2 uM calponin developed approximately three times as much force as unregulated thin filaments with 100% phosphorylated myosin. In the presence of tropomyosin and calponin, the same maximum force was produced with as little as 10% thiophosphorylated myosin. The addition of 3 uM smooth muscle caldesmon under these conditions had no effect on maximum force with 100% phosphorylated myosin, but reduced force by >90% with 20% phosphorylated myosin. These findings demonstrate that caldesmon inhibits the activation of dephosphorylated cross brides by "turned-on" thin filaments, and does so at concentrations lower than those required to inhibit phosphorylated cross bridges.

NUCLEIC ACID MOTIFS FOR PROTEIN RECOGNITION

Th-PM-Sym-1

INTERACTION OF INITIATION FACTORS WITH mRNA. ((D.J. Goss))
Hunter Col., CUNY.

Th-PM-Sym-2

THE IRON REGULATORY ELEMENT (IRE) IN FERRITIN mRNA. ((E.C. Theil, H. Sierzputowska-Gracz, and R.A. M^{c}Kenzie)) **Departments of Biochemistry and Physics, North Carolina State University, Raleigh, NC, 27695-7622.**

Iron storage (ferritin) and iron uptake [transferrin receptor (TfR)] is coordinately regulated in animals by the IREs in mRNA and the IRP regulator protein, a cytoplasmic aconitase (reviewed in Theil, (1994) *Biochem. J.* 304:1-11).Low cellular iron levels enhance IRE/IRP binding to block eIF and ribosome binding (ferritin mRNA) or nuclease binding (TfR mRNA). All IREs are hairpins with a conserved terminal loop (HL), CAGUGU/C . Instability IREs with AU-rich stems, occur as five sets, each one phylogenetically conserved in the 3'-UTR. Translation IREs (erythroid aminolevulinate synthase and ferritin) have more G/C-rich stems and are in the 5'-UTR near the cap. The ferritin IRE is functionally distinct; it is more efficient and encoding both translation enhancement and repression. Structural distinctions of the ferritin IRE include an internal loop , rather than a bulge, and a base paired flanking region with a conserved triplet of base pairs (TBP) 11 nucleotides from the IRE; mutation showed that TBP enhance negative control.

Structure analysis of the ferritin IRE (wild type and mutant) by nuclease cleavage, alkylation, and cleavage by transition metal complexes showed: a hairpin with higher order folding [Fe-EDTA and NMR-^{1}H (pcp and 1 -1) and ^{31}-P], a G-C pair in the HL (nuclease, alkylation, NMR) and heat stable, subdomains (1,10-phen-Cu, Fe-bleomycin, Rh(phen)$_2$Phi^{3+}, NMR, UV-vis). The IRE forms the IRP binding site ("footprint"). G/A mutation in the HL abolished IRP binding and negative, but not positive control. The mutant hairpin melted 10° lower (42°), indicating the importance of the HL in stabilizing the three dimensional shape required to recognize the IRP (part support NIH-DK 20251).

Th-PM-Sym-3

THERMODYNAMIC SIGNATURES OF CONFORMATIONAL CHANGES INDUCED BY SITE-SPECIFIC PROTEIN-DNA ASSOCIATION ((R. S. Spolar & M. Thomas Record, Jr.)) Departments of Chemistry and Biochemistry, University of Wisconsin-Madison, Madison, WI 53706

Site-specific protein-DNA associations are typically accompanied by large negative changes in heat capacity ($\Delta C°$), which we have interpreted in terms of a dominant contribution from the removal of nonpolar surface from water upon complex formation. Since the amount of nonpolar surface involved appears too large to be explained by a "rigid body" association, we proposed that conformational changes in the protein are coupled to binding. To examine this hypothesis further we developed a thermodynamic analysis of the $\Delta C°$ and of the entropy change of binding. Our dissection of the $\Delta C°$ and the entropy change of protein-ligand interactions (including protein-DNA complexation) suggests that local folding or other ordering transitions are coupled to site-specific binding. Numbers of residues predicted by this analysis to fold upon binding generally agree well with structural estimates. Our thermodynamic prediction for protein-DNA complexation parallels a growing body of structural evidence indicating that the conformational transitions which occur upon binding create key parts of the protein-DNA interface. Currently we are dissecting the enthalpic contributions to binding and will discuss the thermodynamic signature of conformational changes in the DNA, in the absence of structure.

Th-PM-Sym-4

INTERACTIONS AND ENERGETICS OF AN RNA HAIRPIN BOUND TO THE U1A RNA-BINDING DOMAIN. ((K.B.Hall)) Washington University School of Medicine, St. Louis, MO 63110

The isolated 102 amino acid N-terminal RNA binding domain (RBD) of the human U1A protein specifically interacts with a short RNA hairpin containing the U1 snRNA stem/loop II sequence. This recognition is nucleotide-specific, for substitutions of critical nucleotides in the RNA loop decrease binding affinity up to 10^6-fold, as measured by nitrocellulose filter binding experiments. The magnitude of the loss of binding free energy with single nucleotide substitution in the conserved GCA sequence suggests that the interaction between the RBD and RNA occurs through a number of interdependent specific contacts in the complex. ^{13}C- and ^{15}N-NMR experiments, using isotopically-labelled RNA together with unlabelled protein, show that the chemical shifts of several nucleotides in the bound RNA are substantially different from those in the free RNA, especially in the loop region of the hairpin. The energetics suggest that there is a large negative heat capacity associated with complex formation, and that the temperature-dependent entropy and enthalpy compensate such that the free energy is relatively constant. These data together suggest that the complex is formed through a concerted rearrangement of the RNA, and probably the protein as well, to form the optimal and base-specific contacts leading to this high affinity and very specific association. The formation of the complex can thus be best described as an induced fit.

NEURONAL CHANNELS

Th-PM-A1

OPTICAL ACTIVITY OF INTACT NERVE BUNDLES. ((David Landowne)) Univ. of Miami Sch. of Medicine Miami, FL 33101.(Spon. by B.Rose)

When photons pass through an organized tissue their polarization is altered due to interactions with the atoms of the tissue. Experimentally the changes in polarization are called 'linear' and 'circular' and are a measure of, respectively, the 2-dim projection and the 3-dim organization of double-bonds in the tissue. With observations at different orientations of the tissue in regards to the light, the symmetry of those measurements must include the symmetry elements of the tissue (Neumann's Principle).

The intensity of light passing through squid fin nerves between crossed linear polarizers was measured with nerves mounted perpendicular to the light path. When intensity is plotted as a function of the azimuth of the long axis of the nerve, four intensity maxima and four minima are seen The minima are not separated by 90° but instead by alternately 87.3°(±0.3°, n = 6) and 92.7°. The smaller angle is roughly symmetric about the long axis of the nerves. In the same apparatus a mica retarder yielded minima separated by 90.1° ± 0.2°. The inhomogeneous Jones matrix

$$\begin{vmatrix} 0.98 + 0.17\,i & 0.01\,i \\ -0.01i & 0.98 - 0.17\,i \end{vmatrix}$$

predicts similarly displaced minima. This is the sum (not the product) of matrices representing linear and circular retardation minus a unit matrix.

The circular retardation produced by the nerves indicates, in spite of the roughly cylindrical appearance, there is no plane of reflection in the average structure of the nerve. A helix lacks this symmetry yet retains the general cylindrical form. Ultrastructural and x-ray observations by others suggest several levels of helical structure within nerves.

Supported by NIH grant NS26651.

Th-PM-A2

ANALYTICAL SOLUTION OF THE ELECTRICAL BEHAVIOR OF BRANCHED PASSIVE DENDRITIC TREES.((I.Z. Steinberg)) Dept. of Neurobiology, Weizmann Institute of Science, Rehovot 76100, Israel.

The spread of electric potential along a uniform passive nerve process can be reconstructed from a sum of pairs of sine and cosine functions of potential vs. distance with proper coefficients (eigenfunctions). Each of the eigenfunctions decays with a rate constant which is related to the wavelength. The challenge is thus the evaluation of the eigenfunctions. The wavelength depends on the boundary conditions of the various segments in the tree, which require continuity of potential, as well as balance of charge flow, at all junctions (Major,G. et al.1993. Biophys.J. 65:423-449). When properly formulated, these boundary conditions lead to a set of homogeneous linear equations in which the coefficients of the sine and cosine functions in the eigenfunctions are the unknowns. These equations have a solution if the relevant determinant vanishes, a condition which permits the evaluation of the wavelengths and decay times which are compatible with the boundary conditions. The various coefficients of the pairs of the sine and cosine functions of a permitted wavelength may then be obtained from the simultaneous equations, thus yielding analytic expressions for the eigenfunctions.

Th-PM-A3

A PUTATIVE NOVEL NA CHANNEL cDNA ISOLATED FROM MOUSE NB2a NEUROBLASTOMA CELLS
((Zheng Fan, Yoshiharu Tokuyama, John W. Kyle, Jonathan C. Makielski)) Department of Medicine, The University of Chicago, Chicago, IL 60637

We have measured whole cell Na currents in mouse NB2a neuroblastoma cells before and after differentiation induced by treatment of cells with media containing DMEM, 1.5% FBS and 1.5% DMSO. Na current density was significantly increased following differentiation with no detectable change in channel kinetics and STX block. To determine the Na channel isoforms expressed in these cells, we isolated mRNA before and after differentiation and used RT-PCR with degenerate primers designed from highly conserved regions of domain IV, which bracketed 460 bp's with divergent sequences among known Na channel α subunits. The PCR products were analyzed by sequencing. In addition to detecting the mouse brain II homolog of rat brain II, we detected a new cDNA sequence which may encode a Na channel isoform. This novel partial cDNA was found both in undifferentiated and differentiated cells, but more frequently in differentiated cells under our experiment conditions. The cDNA is most similar to rat brain II in both nucleotide sequence (~75% identical) and deduced amino acid sequence (~90% identical). Most of the differences in amino acid sequence occurred in the regions of S1-S2 and S5. Using specific primer and RT-PCR, this novel sequence could be detected in human, rat and mouse brain mRNA but not in human heart mRNA. We also sequenced the cDNA clone from rat mRNA, which had a slightly different nucleotide sequence but coded for the identical amino acid sequence as the mouse NB2a clone. These data lead us to propose that the partial cDNA clone that we have isolated from NB2a cells is not the brain II isoform but a novel isoform of Na channel α subunit which is mainly expressed in neurons of mouse and other species.

Th-PM-A4

A NEW MODEL OF *SHAKER* INACTIVATION GATING REQUIRES CLOSED STATE INACTIVATION TO DESCRIBE I2 KINETICS. ((R.K. Ayer, Jr., L. Lin and F. Sigworth)) Dept. of Cell and Molec. Physiol., Yale Univ. Sch. of Med., 333 Cedar St., New Haven CT. 06510.

In a previous report (McCormack et al., 1993, Biophys J. 65:1740-48), hydrophobic substitutions at *Shaker* L382, located at the end of the S4 region, were shown to produce large shifts in the voltage dependence of activation and inactivation. Generally, each mutation shifted the voltage dependence of the two parameters by similar amounts; this is expected if inactivation is coupled to activation. The isoleucine substitution (I2) does not follow this rule; while activation is shifted by 45mV, inactivation is shifted by only 10mV. This suggests that inactivation has become uncoupled from activation in I2 (Ayer et al., 1993, Biophys. J. 64:A114).

We will present details of a new model that describes the macroscopic kinetics of inactivating wildtype (WT) and I2 channels. Briefly, while WT currents can be fit by a voltage independent inactivation process that progresses only from the open state, I2 kinetics require adding inactivation from closed states. This result is consistent with the S4-S5 linker being involved in inactivation (Isacoff et al., 1991, Nature. 353:86-90).

We will also describe experiments that used trypsin to remove the inactivation gate of WT and I2 channels expressed at high density in macropatches. WT peak current increases at threshold voltages after trypsin treatment; this is expected for a channel with inactivation occurring at a constant rate from the open state. I2 current increases by 50 to 100% at all voltages, again suggesting channels can inactivate without opening. The new model predicts the I2 and WT current increases seen after enzyme treatment.

Th-PM-A5

MOLECULAR DETERMINANTS OF SODIUM CHANNEL INACTIVATION INCLUDE RESIDUES NEAR SEGMENT IS6. ((J.-F. Zhang, P.T. Ellinor, R.W. Tsien and R.W. Aldrich)). Dept of Mol & Cell Physiol, HHMI, Stanford University, Stanford, CA 94305.

We have previously found that the inactivation of voltage-gated Ca^{2+} channels is strongly dependent on a region of the α_1-subunit that includes segment IS6 and neighboring residues in putative extracellular and cytoplasmic loops (Zhang et al., *Nature*, in press). The inactivation shows considerable resemblance to C-type inactivation in K^+ channels. Our results for Ca^{2+} channels were unexpected in light of the current view of inactivation in Na^+ channels, and they raise obvious questions about Na^+ channel inactivation in light of sequence homologies between Na^+ and Ca^{2+} channels. Accordingly, we have made chimeras between two skeletal muscle Na^+ channel α-subunits displaying slowly inactivating (μ1) and rapidly inactivating (SKM2) characteristics. The chimeras and parental channels were expressed in *Xenopus* oocytes in whole cell recordings with 100 mM Na^+ as the external charge carrier. Chimera μ1-7 was constructed by transferring a segment near IS6 from SKM2 to μ1 (inset). It inactivates faster than the parental μ1 channel (5.0±0.7 vs 8.4±0.3 ms, single exp fit, Vt = 0 mV). While illustrated in the absence of β-subunits, the acceleratory effect of the substitution was also seen in their presence. These results suggest that in Na^+ channels, as in Ca^{2+} channels, inactivation is strongly affected by the nature of the residues near IS6.

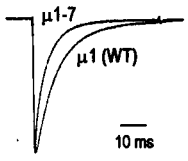

Th-PM-A6

SINGLE VOLTAGE-ACTIVATED NA^+ AND K^+ CHANNELS IN THE SOMATA OF VISUALLY IDENTIFIED MOTONEURONES STUDIED IN THIN SLICES OF RAT SPINAL CORD: COMPARISON WITH AXONAL CHANNELS ((B.V. Safronov & W. Vogel)) Physiologisches Institut, Justus-Liebig-Universität Giessen, Aulweg 129, 35392 Giessen, Germany

Voltage-activated Na^+ and K^+ channels were investigated in the soma membrane of motoneurones by means of the patch clamp technique applied to thin slices of neonatal rat spinal cord.

One type of TTX-sensitive Na^+ channel with a conductance of 14 pS was found to underlie the Na^+ conductance in the soma of motoneurones. The channels were activated within a potential range between -60 and -20 mV. The kinetics of Na^+ channel inactivation could be fitted with a monoexponential function (1-4 ms) at all potentials investigated. Kinetics of recovery of Na^+ channels from inactivation at a potential of -80 mV were double-exponential with a fast component of 16 ms (76%) and a slow one of 154 ms (24%).

The whole-cell K^+ currents consisted of transient (A) and delayed-rectifier (DR) components. The most frequent single K^+ channel found in the soma of motoneurones was the fast inactivating A-channel with a conductance of 19 pS in external Ringer. In symmetrical high-K solutions the conductance was 51 and 40 pS for inward and outward currents, respectively. A-channels activated between -60 and +20 mV. In high-K_o solution A-channels deactivated rapidly at potentials between -110 and -60 mV.

K^+ DR-channels were found in the soma membrane at a moderate density. The channel conductance in Ringer was 10 pS and in symmetrical high-K solutions it was 31 and 23 pS for inward and outward currents, respectively. The channels activated at -60 to 0 mV. In external high-K_o solution DR-channels showed slow deactivation kinetics.

Uneven distribution of the channels investigated is discussed. Na^+ and K^+ channels found in the somata of motoneurones are compared with one Na^+ and three types of voltage-activated K^+ channels described previously in the myelinated axons.

Th-PM-A7

FUNCTIONAL EXPRESSION OF THREE K CHANNEL β-SUBUNITS. ((Stefan H. Heinemann[1], Jens Rettig[2,3], Olaf Pongs[2]))
1: Max-Planck-Gesellschaft z.F.d.W. e.V. AG Molekulare und zelluläre Biophysik, D-07747 Jena, Germany; 2: Zentrum für Molekulare Neurobiologie Hamburg, Institut für Neurale Signalverarbeitung, D-20246 Hamburg, Germany. 3: Present addr.: Dept. Pharmacology, Univ. Washington, Seattle, WA 98195.

A potassium channel β-subunit from rat brain (Kvβ1) was recently shown to induce fast inactivation of potassium channels from the Kv1 family (Rettig et al., Nature, 369, 289-294, 1994). The mechanism of this inactivation is similar to the N-type inactivation of A-type channels. In this case, however, the N-terminal end of the β-subunit acts as the inactivating domain. A new β-subunit (Kvβ3) was cloned from rat brain; it is a protein of 403 amino-acid residues with a 68% amino-acid sequence homology to Kvβ1. This subunit also has a long N-terminal structure and induces inactivation in channels of the Kv1 family. However, the inactivation is not as complete as that obtained by coexpression of Kvβ1. Similarly to Kvβ1 the Kvβ3-induced inactivation is regulated by the intracellular redox potential. The second member of the β-subunit subfamily, Kvβ2, has a shorter N-terminal end and does not cause inactivation when coexpressed with channels of the Kv1 family. To test whether this subunit actually coassembles with the α-subunits, the N-terminal ends of Kvβ1 and Kvβ3 were spliced to the N-terminus of Kvβ2. These constructs did induce fast inactivation of Kv1 channels, indicating that Kvβ2 associates with the α-subunits.

Th-PM-A8

CONTRIBUTION OF THE SPATIAL DISTRIBUTION OF Ca^{2+}-DEPENDENT POTASSIUM CHANNELS AND Ca^{2+} CHANNELS TO THE TIME COURSE OF I_{AHP} IN NGF-TREATED CULTURED BULLFROG SYMPATHETIC GANGLION NEURONS. ((S.D. Hocherman and P.R. Adams)). SUNY at Stony Brook, NY 11794-5230.

In previous work (Hocherman and Adams (1994), Biophys. J. 66: A327) it has been shown that bullfrog sympathetic neurons lose most of their long afterhyperpolarization upon dissociation, and that in whole cell measurements its underlying current (I_{AHP}) decays faster than in measurements with perforated patches or sharp microelectrodes. This current recovered after a few days in culture at room temperature in the presence of nerve growth factor (NGF) in cells that developed neurites. In addition, the time constant of decay slowed down in whole cell measurements and the number of action potentials needed to activate half of the maximal current decreased, implying an increase or redistribution of Ca^{+2} channels as well as an increase in Ca^{2+}-dependent K^+ channels. We are currently examining the hypothesis that the slowing of the kinetics of the decay of the I_{AHP} in whole cell measurements is a result of redistribution of both Ca^{2+} and K^+ channels in the cell. The presence of Ca^{2+} channels in the neurites was inferred from confocal measurements of Ca^{2+} transients, and it was also suggested from voltage clamp measurement of Ca^{2+} currents in the soma. The presence of Ca^{2+}-dependent K^+ channels in the cell body as well as in the neurites was directly monitored by dual electrode recording. While one electrode measured the total I_{AHP} in whole cell configuration, a second electrode was used in cell attached mode to probe for the presence of single channels, either in the cell body or in the neurites. A small channel, with conductance of roughly 20 pS, was activated following a train of action potentials and deactivated slowly at V=-55 or V=-85. The time course of the ensemble average of the single channel activity did not closely follow the time course of the whole cell current, suggesting regional asymmetries in the channel distributions and/or the presence of restricted space for diffusion of Ca^{2+} ions.

Th-PM-A9

FUNCTIONAL COUPLING BETWEEN L-TYPE CALCIUM CHANNELS AND CAFFEINE-SENSITIVE CALCIUM STORES IN CEREBELLAR GRANULE CELLS. ((P. Chavis, L. Fagni, J. Bockaert, and J.B. Lansman))
Department of Pharmacology, UCSF School of Medicine, San Francisco, and CCIPE-UPR, Montpellier Cedex-5 France

Metabotropic glutamate receptors (mGluR) activate two distinct signaling pathways in mouse cerebellar granule cells. One pathway is activated by the mGluR2, R3 subtypes and inhibits currents through N- and L-type Ca channels. This pathway is slow, blocked by pertussis toxin and not reversible. A second, previously unrecognized pathway, is activated by the mGluR1, R5 subtypes and produces a large, oscillatory increase in the current through L-type Ca channels. This pathway is rapid, pertussis toxin-insensitive, and reversible. We studied the oscillations of the whole-cell Ca currents in experiments in which a 50 ms voltage step was continuously applied to the cell at a rate of 2/sec. After exposure to the mGluR agonist, t-ACPD (400 μM), the amplitude of the depolarization-evoked Ca current increased abruptly; it then decreased during successive voltage steps, but, subsequently, increased again. This pattern persisted throughout exposure to t-ACPD and had a period of ~.1 Hz. The oscillations were not blocked with high intracellular Ca buffering or inhibitors of phosphorylation. We found, however, that caffeine (20 mM) triggered the Ca current oscillations in the absence of t-ACPD. Ryanodine (10 μM) inhibited the oscillations produced by either t-ACPD or caffeine after several cycles, consistent with its use-dependent blocking actions. We suggest that activation of Ca-induced Ca release triggers the Ca current oscillations by mechanism which involves close coupling between the intracellular Ca stores and L-type Ca channels in the cell membrane. Coupling may provide a mechanism for capacitive Ca entry into neurons.

Th-PM-A10

ELEMENTARY PROPERTIES OF TWO NON-L-TYPE Ca^{2+} CHANNELS IN FROG SYMPATHETIC NEURONS. *((B.A. Lewis, Jr, S. Dubel, T.W. Soong, T.P. Snutch and D.T. Yue)), Johns Hopkins University, Baltimore, MD 21205.*

Gaining molecular information about N-type Ca^{2+} channels is of particular importance because of their role in neurotransmitter release. One of the preparations of choice in the study of N-type calcium current has been the bullfrog sympathetic neuron (FSN), which was assumed to contain only L- and N-type channels. But now evidence suggests that a third type of Ca^{2+} channel may exist (Elmslie, *et.al., Neuron* 13:217). This may require revision about presumed elementary properties of N-type Ca^{2+} channels. Here we extend single-channel evidence for a novel Ca^{2+} current. Using FPL-64176 to screen out patches with L-type Ca^{2+} channels, voltage steps ranging from -20 to 30 mV reveal currents with unitary conductances of 12-pS and of 18-pS which are, respectively, insensitive and sensitive to ω–conotoxin GVIA (ω-Cgtx) incubation. Voltage ramps of these single-channel patches further show that the ω-Cgtx-insensitive ("novel") channel begins to activate at -30 mV and is mostly inactivated at holding potentials -40 mV or greater. Under the same voltage protocol, the ω-Cgtx-sensitive (N-type) channel starts to open at 0 mV and is less sensitive to holding potential. Three-dimensional amplitude histograms of ramp data -- compiled with respect to voltage as well as current -- demonstrate the development of two distinct open distributions during the depolarization. We correlate these findings with B- and E-class Ca^{2+} channel clones expressed in HEK-293 cells. The unitary current-voltage relationship of the E-class channel overlaps with that of the "novel" FSN channel. Futhermore, as evaluated using conditional open probability analysis, both the E-class and "novel" channels exhibit reversible uncoupling of inactivation -- a property first attributed to the N-type (Plummer and Hess, *Nature* 351:657). In contrast, the B–class and N-type channel have similar unitary current properties, and neither channel exhibits reversible uncoupling of the sort described by Plummer and Hess. We argue that the "novel" channel expressed in FSN belongs to the class E. Reverse-transcriptase polymerase chain reaction (RT-PCR) cloning is under way to confirm this further.

Th-PM-B1

A RESIDUE IN THE C-TERMINAL DOMAIN IS CRITICAL FOR GATING IN AN INWARD-RECTIFIER K^+ CHANNEL ((J. Yang, Y.N. Jan and L.Y. Jan)) Dept. of Physiol., HHMI, UCSF, San Francisco, CA 94143. (Spon. by J. Finer-Moore)

Inwardly rectifying K^+ channels conduct inward K^+ flux more efficiently than outward flux, a property important for their biological functions. The major mechanism for this inward rectification is voltage-dependent blockade by intracellular Mg^{2+} and other diffusible factors (Lopatin et al., J. Physiol., 477, 86P (1994)). In the strongly rectifying IRK1 channel, mutation of an aspartate residue in the second transmembrane domain has been shown to affect Mg^{2+} binding and "intrinsic gating" (Stanfield et al., J. Physiol., 478, 1-6 (1994); Wible et al., Nature, 371, 246-249 (1994)) - now attributed largely to blockade by the diffusible factors. However, the mutant channels still exhibited strong rectification similar to that in the wild-type channel, indicating the involvement of other regions in channel gating. We have identified a negatively charged residue, E224, in the putative cytoplasmic C-terminal domain that appears to be critical for gating in IRK1. Mutation of this residue produced channels that conduct significant transient as well as small sustained outward K^+ current. Mg^{2+} affinity was reduced from ~40 μM (+40 mV) in wild-type to ~120-2000 μM in mutant channels. The affinity for a diffusible factor was decreased even more, by as much as >1000-fold. The potency of the mutations depends on the chemical nature as well as size of the side chain of the substituting residue. Some mutant channels showed strong inward rectification independent of Mg^{2+} and diffusible factor block. Furthermore, some mutant channels demonstrated very rapid flickering single-channel openings and reduced single-channel conductance. Thses results suggest that in IRK1 part of the C-terminal domain participates in forming the channel pore and plays a critical role in channel gating.

Th-PM-B2

STRONG INWARD RECTIFICATION OF INWARD RECTIFIER K^+ CHANNELS IS CAUSED BY INTRACELLULAR POLYAMINES

((B. Fakler, U. Brändle, E. Glowatzki, H.-P. Zenner and J. P. Ruppersberg)) Dept. of Sensory Biophysics, ENT-Hospital of the University of Tübingen, Röntgenweg 11, 72076 Tübingen, Germany

Inward rectifier K^+ channels mediate the K^+ conductance at resting potential in many types of cell. Since these K^+ channels do not pass outward currents (inward rectification) when the cell membrane is depolarized beyond a trigger threshold, they play an important role in controlling excitability. Both a highly voltage-dependent block by intracellular Mg^{2+} and an endogenous channel gating process are presently assumed to underlie inward rectification. Using the giant patch-clamp technique in cell-attached and inside-out configuration we show that the strong voltage-dependence of inward rectifier K^+ channels found under physiological conditions is due to multiply charged intracellular polyamines such as spermine (SPM) and spermidine (SPD). Under physiological conditions, IRK1 inward rectifier K^+ channels are blocked by SPM with an affinity of 24 nM (at +50 mV membrane potential), far beyond the affinity for Mg^{2+}. Probing the spermine-sensitivity of three other cloned inward rectifier K^+ channels revealed that BIR11 (97% identity in amino acid sequence with MB-IRK3) and BIR10 were efficiently blocked by SPM but their sensitivity was more than ten times lower than for IRK1, and ROMK1 was about 100 times less sensitive to SPM, correlating well with its less pronounced rectification properties.

Th-PM-B3

GATING OF INWARD RECTIFIER K^+ CHANNELS CAN BE PRODUCED BY INTRACELLULAR POLYAMINES. ((E. Ficker, *M. Taglialatela, B.A. Wible, *C.M. Henley and A.M. Brown)) Dept. of Molecular Physiology & Biophysics, *Dept. of Otorhinolaryngology, Baylor College of Medicine, Houston, TX 77030 and *Dept. of Neurosciences, University of Naples, 80121 Naples, Italy. (spon. by M. Taglialatela)

Inward rectifier K^+ channels (IRKs) conduct preferentially inward currents while outward currents are largely blocked. Two mechanisms of inward rectification have been described: a fast, time-independent block by intracellular Mg^{2+} and a slower, time-dependent and Mg^{2+}-independent "intrinsic" gating. In cloned IRKs, time-dependence has been localized to an Asp residue in the second putative transmembrane domain M2 (D172 in IRK1). The time-dependence of IRK currents expressed in *Xenopus* oocytes is rapidly lost upon patch excision suggesting the involvement of cytoplasmic factors. Time-dependent gating can be restored in excised patches by nanomolar concentrations of two naturally occurring polyamines (PAs), spermine (SPM) and spermidine (SPD). Substitution of the Asp 172 for Asn in IRK1 decreased channel affinity for SPM and SPD. Putrescine (PUT) produced fast, time-independent block of both IRK1 and IRK1 D172N. Accordingly, the reciprocal mutation in ROMK1 channels (N171D) increased the affinity for SPD by 10^4-fold, thereby introducing time-dependent gating. The proposed role for PAs as physiological modulators of IRKs is further supported by the finding that the levels of PAs determined fluorimetrically in *Xenopus* oocytes are compatible with those required to block IRK1 channels. In conclusion, we propose that what has been referred to as "intrinsic" gating may largely reflect voltage-dependent block by organic cations such as SPM and SPD.

Th-PM-B4

GIRK BURST OPEN PROBABILITY IS A FUNCTION OF THE NUMBER OF BOUND G PROTEIN SUBUNITS. ((T.T. Ivanova and G.E. Breitwieser)) Dept. of Physiol., Johns Hopkins Univ. Sch. of Med., Baltimore, MD 21205.

Muscarinic receptor-activated K^+ channels (GIRK) open in response to direct interaction with subunits of activated G proteins. Molecular cloning has revealed a homotetrameric structure, providing 4 potentially equivalent binding sites for G protein subunits. To determine whether GIRK gating can occur with less than 4 G protein subunits bound, burst analysis on one-channel patches was performed. Patches (from bullfrog atrial myocytes) were excised into 1 mM AppNHp, then exposed to 100 μM GTPγS. Analysis revealed that bursts were distributed into defined open probability ranges, well-fitted with the sum of 4 γ functions. We interpret these results to indicate that the GIRK open probability in any given burst is determined by the number of bound G protein subunits. Further, the most probable state or mode in the presence of GTPγS is that in which 3 G protein sites are occupied, suggesting that the cellular level of G protein may be limiting. The average burst duration was constant (approx. 260 ms), and not a function of the open probability within the burst. Further, burst duration was not affected by the guanine nucleotide used to activate the G protein (GTPγS or GTP), suggesting that GTP hydrolysis does not limit burst duration. These results are consistent with termination of the burst being the result of GIRK channel entry into a non-active state despite the presence of bound G proteins. Supported by AHA and NIH.

Th-PM-B5

G PROTEIN ACTIVATED K^+ INWARD RECTIFIER (GIRK1): POSSIBLE ROLE OF C-TERMINUS IN GATING AND ACTIVATION BY G PROTEIN βγ SUBUNITS. (N. Dascal*, W. Schreibmayer#, T. Ivanina*, C. Doupnik¶, C. Chavkin¶, H.A. Lester¶, N. Davidson¶) *Dept. Physiol. & Pharmacol., Tel Aviv University Medical School, Tel Aviv 69978, Israel; #Institute of Medical Physics and Biophysics, Graz University, A8010 Graz, Austria; ¶Division of Biology 126-29, Caltech, Pasadena, CA 91125, USA.

The last 160 amino acids (a.a.) at the (presumably) cytoplasmic C-terminal side of the 501 a.a.-long GIRK1 are unique and may participate in direct binding of the βγ subunits of G proteins, mediating the neurotransmitter-induced activation of the channel. GIRK1 was coexpressed with the muscarinic m2 receptor in *Xenopus* oocytes. A mutant channel $GIRK1_{1-341}$ lacking the C-terminal 160 a.a. still showed an ACh-induced current, reduced by 75% as compared to WT. In excised patches, both WT channel and $GIRK1_{1-341}$ were activated by purified $\beta_1\gamma_2$ subunits, suggesting that βγ binding site is not entirely contained within the C-terminal 160 a.a. We constructed a DNA ($GIRK1_{183-501}$*src*) coding for the whole C-terminal part of the channel (starting directly after the second transmembrane segment), with an N-terminal stretch that allowed myristoylation of the resulting protein, driving its attachment to plasma membrane. The localization and relative amounts of the expressed full-length channel and of $GIRK1_{183-501}$*src* in cytosol and in plasma membrane have been verified by SDS-PAGE in [^{35}S]methionine labeled oocytes. Current via the WT GIRK1, but not via a voltage-dependent *Shaker* B channel, was reduced by coexpression of excess of $GIRK1_{183-501}$*src* (by 70%), supporting the idea that it binds βγ and competes with the full-length channel for the available βγ. However, the current via an inwardly rectifying channel that is not known to be regulated by G proteins, ROMK1, was reduced by 50% by coexpression of $GIRK1_{183-501}$*src*, suggesting that the C terminus of GIRK1 may contain a stretch whose function is to block the ion permeation pathway. The quest for mechanisms of block and of activation of GIRK1 by βγ is in progress. Supported by NIH, BSF USA-Israel, Austrian National Bank, and HFSP.

Th-PM-B6

IDENTIFICATION OF CYTOPLASMIC STRUCTURES INVOLVED IN ACTIVATION OF THE MUSCARINIC POTASSIUM CHANNEL (GIRK1) BY Gβγ SUBUNITS. ((Slesinger, P.A., Huang, C.L., Reuveny, E., Jan, Y.N. and Jan, L.Y.)) Dept. of Physiology and HHMI. UCSF, San Francisco, CA 94143

Activation of the atrial muscarinic potassium channel (GIRK1) is important in the regulation of the heart beat and occurs through a membrane-delimited interaction with G-proteins. We showed previously that Gβγ subunits of the G-protein trimer are sufficient to activate GIRK1 (Nature, 1994). Based on the limited homology between C terminus of GIRK1 and the βγ-binding domain of βARK1, we proposed that the C terminus of GIRK1 interacts with Gβγ. To determine which regions of GIRK1 interact with Gβγ, we constructed fusion proteins of cytoplasmic segments of GIRK1 and tested for binding with Gβγ. Co-precipitation assays indicated that the entire C terminus of GIRK1 but not of the G-protein insensitive IRK1 binds Gβγ. Deletions of the C terminus narrowed the region involved to ~100 amino acids. A synthetic peptide derived from this region of the C terminus of GIRK1 partially inhibited Gβγ activation of GIRK1 single-channel activity measured in excised patches, suggesting that this region is physiologically important in the activation of GIRK1. This ~100 amino acid segment of the C terminus is contained within the region of the C-terminus shown to be homologous with the βγ-binding domain of βARK1. Surprisingly, co-precipitation assays also suggested that Gβγ binds to the N-terminus but not as well as the C-terminus. We are currently examining whether binding to the N-terminus is physiologically important.

Th-PM-B7

CYTOPLASMIC PROTON AND Ca^{2+} POTENTLY BLOCK THE ROMK1 K^+ CHANNEL EXPRESSED IN COS CELLS: IMPLICATION OF A SELECTIVE CATION REGULATORY SITE(S).((J. Wang, L. Cipkus Dubray, M.E. Shuck, M.J. Bienkowski, V. E. Groppi and K. S. Lee)) Cardiovascular Pharmacology and Cell Biology, The Upjohn Company, Kalamazoo, MI 49002.

We have shown earlier that intracellular acidification potently blocked the ROMK1 channel expressed in *Xenopus* oocyte. Here we report that ROMK1 K^+ channel stably expressed in the COS cells was sensitive to submicromolar concentrations of intracellular proton and Ca^{2+}. Single channel ROMK1 currents were recorded in symmetrical 140 mM K^+, Cl^--free solution using the cell-attach or inside-out configuration. In cell-attach mode, the averaged single channel conductance was 30 pS with occasional sub-conductance states detectable. The inward current amplitude negative to E_K was linear with voltage, but the outward current positive to E_K rectified strongly inward. The channel had a high open probability (P_o) of 0.8 that was not sensitive to voltage negative to 0 mV, with two time constants for both open (1.3 and 15.5 ms) and closed (0.2 and 1.3 ms) states. It was blocked by 0.5 mM Ba^{2+} in the pipette. Internal acidification from pH 7.4 to 6.5 using acetate buffer completely inhibited channel activity with a pK of 6.8. In inside-out mode, patch excision to Mg^{2+}-free solution significantly reduced or abolished the inward rectification. More importantly, in the same solution at pCa 9, reducing pH from 7.5 to 6.75 reduced ROMK1 P_o from averaged 0.64 to 0.09; increasing pCa from 9 to 7, with pH kept constant at 7.2, also decreased averaged P_o from 0.72 to 0.2. The unique pH and Ca^{2+} sensitivity of ROMK1 in the physiological range may suggest that this kidney channel is closely regulated by a highly sensitive, cation binding site(s).

Th-PM-B8

DUAL GATING MECHANISMS IN *H-ERG* K^+ CHANNELS: INWARD RECTIFICATION AND "S4-LIKE" VOLTAGE DEPENDENCE. ((Gail A. Robertson and Matthew C. Trudeau)) Dept. of Physiology, University of Wisconsin, Madison, WI 53706.

We have expressed the *h-erg* gene in frog oocytes and found that it encodes an inwardly rectifying K^+ channel, despite its homology to the outwardly rectifying members of the *eag* family. Like other inward rectifiers, activation of *h-erg* occurs at voltages negative to E_K, consistent with a blocking particle gating mechanism (Trudeau et al., this vol.). Although these channels are activated by hyperpolarizing voltages, the number of channels available for activation is regulated by the prepulse voltage. This dependence of conductance on prepulse voltage can be fitted with a Boltzmann relation, giving a voltage of half-maximal activation of 4 mV and a slope factor of 14 mV per e-fold change in conductance. The values of these parameters are similar to those describing the voltage dependence of activation of outwardly-rectifying *eag*-related channels. The correspondence of these measurements may reflect conserved gating mechanisms, such as S4-mediated conformational transitions that precede channel opening during depolarization. In the case of *h-erg* channels, the "open" channel would be blocked internally, and activation would reflect the alleviation of the blocking particle as K^+ ions flow into the cell.
Funded by the American Heart Association of Wisconsin.

PROTEINS II

Th-PM-C1

ROLE OF WATER IN PROTEIN FUNCTION AND STRUCTURE. ((R.M. Stroud & J.S. Finer-Moore)) Dept. of Biochemistry & Biophysics, UCSF, San Francisco, CA 94143-0448.

A detailed analysis of water associated with proteins has led to a prediction of site where water can be found associated with protein. This can be important both in protein prediction, and important for drug design based on locations of some of these water molecules. By x-ray and neutron crystallography, water molecules associated with the serine proteinase trypsin have been defined extremely accurately. Orientations of the water molecules have been determined and rules for their positional disposition determined. In the enzyme thymidylate synthase, water molecules play a key role in catalysis. At two positions in the reactive cycle, they present pKa's tuned to reaction chemistry. Thus ordered water fulfills a key role as a base and subsequently a different water acts as an agent to stabilize the transition state in the chemical reaction. Chemical structures and three-dimensional structure determinations along the reaction pathway have led to a detailed picture of catalysis by thymidylate synthase. The enzyme involves large conformational changes, reorganization of water molecules and depends on water as a key catalytic ingredient. The mechanism of methyl transfer by thymidylate synthase is also determined in the course of these studies. This represents a most critical role for water in the catalytic mechanism of an enzymatic reaction.

Th-PM-C2

The 2.8Å CRYSTAL STRUCTURE OF THE GRO-ES CO-CHAPERONIN SUGGESTS A NOVEL MECHANISM FOR GRO-EL/GRO-ES ASSISTED PROTEIN FOLDING. ((J.F. Hunt, A.Weaver, S. Landry, L. Gierasch, and J. Deisenhofer)) University of Texas Southwestern Medical Center, Dallas, TX.

We have determined the crystal structure of the GroES co-chaperonin from *E. coli* at 2.8Å resolution. Each GroES monomer forms an anti-parallel β-barrel with a single β-hairpin extending out from one end. The structure of the GroES heptamer resembles a dome. The individual β-barrels are arranged in a ring to form the side wall of the dome while the β-hairpins extend in over the top of the dome to form the roof which can be described as a 7-fold β-pinwheel. The "mobile loop" segment of GroES, previously identified as a GroEL binding determinant, extends from the outer lower rim of the dome, suggesting that the GroES dome sits over the top of the central polypeptide binding cavity in GroEL (an inference consistent with the results of EM image reconstruction studies). The observed structure of the GroES protein suggests a novel hypothesis for the mechanism of GroEL/GroES assisted protein folding which we call the "Check Valve Hypothesis". Specifically, GroES could function as a valve on a polypeptide "pump" formed by the GroEL cylinder. During the "stroke" of the GroEL pump, the roof of the GroES dome could open to allow extrusion of the non-native polypeptide from the binding cavity. While the GroEL pump is in the high-energy, fully compressed state, the β-hairpin extending from each of the GroES subunits could return to its position in the native structure, and the partially extruded polypeptide could still pass through the 8Å orifice in the center of the β-pinwheel. However, the relatively narrow diameter of this orifice could prevent the retraction of the polypeptide back into the binding cavity of GroEL during relaxation of the GroEL pump.

Th-PM-C3 *(Presented at Tu-AM-G10)*

PATHWAYS IN THE SPONTANEOUS AND GROEL-ASSISTED REFOLDING OF GLUCOSE-6-PHOSPHATE DEHYDROGENASE ((John E. Hansen and Ari Gafni)) Department of Biological Chemistry and Institute of Gerontology, University of Michigan, Ann Arbor, MI 48109-2007.

Efficiency of the GroEL-assisted reactivation of bacterial glucose-6-phosphate dehydrogenase (Glu-6-PDH) is temperature dependent. A switch from enhanced to fully arrested reactivation occurs over a narrow temperature range - from 25° to 30° C. This was employed in the current study to trap intermediates from both the spontaneous and GroEL-assisted refolding of Glu-6-PDH. Renaturations were initiated at 2° C to slow down the refolding process allowing to more easily follow individual folding intermediates. At various times following the inception of renaturation the temperature was quickly increased to 35° C, having added GroEL either at the inception of renaturation (for the case of assisted refolding) or immediately before increasing the temperature (for the case of spontaneous refolding), thereby using GroEL to trap folding intermediates. After a delay time the temperature was reduced to 20° C and the fraction of folding intermediates entrapped by GroEL and able to resume renaturation was determined. By measuring the limiting yields of reactivation following these temperature changes and comparing the results with the time courses for spontaneous and assisted reactivation, those folding intermediates that interact with GroEL at a particular temperature were determined. From these studies we have identified three folding pathways in the spontaneous renaturation. In the assisted renaturation, in contrast, GroEL directs the folding along only two of those pathways.

Th-PM-C4

FOLDING OF OUTER MEMBRANE PROTEIN: TWO-STEP MECHANISM ((Natalia A. Rodionova and Lukas K. Tamm*))
Department of Chemistry, New York University, New York, NY 10003 and *Department of Molecular Physiology and Biological Physics, University of Virginia, Charlottesville, VA 22908

The outer membrane protein A (OmpA) constitutes a useful model for membrane protein folding studies because it is soluble in 8 M urea and can be refolded into its native structure in the presence of preformed target lipid bilayers. Native OmpA is thought to form an 8-stranded beta-barrel inserted into the membrane. The insertion of OmpA into lipid bilayers was studied by fluorescence spectroscopy and limited proteolysis. The adsorbed/partially inserted form of OmpA was found below the chain melting phase transition of the lipid. It is distinguished from native (fully inserted) form by a shift in the apparent molecular mass from 35 kDa to 30 kDa on SDS gels. The partially inserted form is digested by trypsin to several minor fragments whereas trypsin digestion of the inserted form of OmpA yields a well defined membrane-protected 24 kDa fragment. We show that a partially inserted form of OmpA that has been identified when the protein was bound to lipid bilayers in the gel phase is also found when the protein is bound to fluid phase lipid bilayers at low temperatures. We demonstrate that the protein in this form become fully inserted upon raising the temperature. The binding kinetics show that the partially inserted form is formed very rapidly, whereas several hours are reguired to fully inserted OmpA into the membrane and generate the native structure of protein. These results suggest that partially inserted form is a kinetically trapped folding intermediate that can be "chased" into the native form simply by raising the temperature.

Th-PM-C5

TIME-RESOLVED RAMAN SPECTROSCOPY OF VIRUS ASSEMBLY.
((R. Tuma and G. J. Thomas, Jr.)) Cell Biology and Biophysics, School of Biological Sciences, University of Missouri, Kansas City, MO 64110.

We are developing time-resolved Raman spectroscopy to monitor the dynamics of assembly of viral capsids and to probe assembly related structural transitions of the capsid subunits [K.E. Reilly & G.J. Thomas, Jr. (1994) *J. Mol. Biol.* 241:68-82]. Here, we describe the theory, design and implementation of a dialysis flow cell for Raman applications to spheroidal bacteriophages PRD1 and ϕ6. The flow cell device facilitates collection of the Raman spectrum while solvent and small solutes (< 1 kDa) are rapidly exchanged accross a dialyzing membrane which is impermeable to protein subunits (> 10 kDa) and virions. A diffusion model quantitatively accounts for experimentally observed exchange rates of solvent and solute species in solutions of viruses and precursor particles. The same mathematical model satisfactorily simulates observed second-order hydrogen-isotope exchanges of capsid subunits and packaged genomes which occur with D_2O as the dialyzing effluent. Deuterations of peptide main chains (NH → ND), selected side chains, and nucleic acid bases (imino NH → ND and amino NH_2 → ND_2) are assigned by analogy with results obtained on model polypeptides and polynucleotides. Factor analysis of the time-resolved Raman spectra enables interpretation of the peptide exchange kinetics in terms of hydrogen bonding sub-states in coat protein subunits. Applications to assembly mechanisms of ϕ6 and PRD1 will be described.
[Supported by NIH Grant GM 50776.]

Th-PM-C6

HOMOTRANSFER FLUORESCENCE STUDY OF TRANSCRIPTION TERMINATION FACTOR RHO SUBUNIT EXCHANGE KINETICS.
((Amy P.S. Chung and S.E. Seifried)) Department of Biochemistry and Biophysics, University of Hawaii, Honolulu, HI 96822.

The transcription termination factor rho of *E. coli* will interact with newly synthesized RNA chains and bring about transcript release from elongation complexes. Rho first binds to a loading site on RNA, then moves along the RNA chain in an ATP-driven RNA binding and release process. When the RNA polymerase elongation complexes reach a pause site the rho can catch up and interact with the transcription bubble and bring about the release of the transcript. This RNA-DNA helicase activity is also driven by RNA dependent ATPase activity. Rho is a hexamer of identical subunits arranged as a trimer of dimers with D3 symmetry. In this study we examine the effects of various parameters on rho subunit exchange rates via homotransfer polarization fluorometry. Parameters varied include temperature, salt concentration and the presence of poly(rC), poly(dC), and ATP. This study supports an existing model of rho subunit exchange, quantitates that exchange, and helps describe the translocation and helicase activities of rho.

Th-PM-C7

EFFECT OF THE N-CAPPING BOX ON STABILITY AND FOLDING OF DOMAIN E OF STAPHYLOCOCCAL PROTEIN A.
((E.A. Zhukovsky, M.G. Mulkerrin, and L.G. Presta))
Depts of Protein Engineering and Medicinal and Analytical Chemistry, Genentech, Inc., South San Francisco CA 94080. (Spon. by M.G. Mulkerrin)

In our previous study (*Biochemistry* 33, 9856-9864 (1994)) we evaluated the contribution of the N-capping box to protein stabilization in hGH. The N-capping box contributed at least 1.5 kcal/mol to protein stabilization and did not dramatically affect the global fold of hGH. hGH is an extremely stable protein (ΔG_U = 14kcal/mol). The next logical step is a test of the effect of the N-capping box on the stabilization and folding of a protein which possesses very low intrinsic stability.

Domain E of staphylococcal protein A is a marginally stable protein (ΔG_U = 2 kcal/mol). We employed site-directed mutagenesis to eliminate interactions characteristic of the N-capping box in helix 2. Far UV CD spectroscopy was used to monitor changes in folding; equilibrium denaturation evaluated changes in stability of the mutants. We find that the hydrogen bond provided by the N-capping residue, Asn21, contributes approximately 0.9 kcal/mol of stabilization energy. However, elimination of all hydrogen bonds comprising the N-capping box results in partial unfolding of the protein, as determined by the far UV CD spectroscopy. This unfolding is reversible and lowering the temperature increases the mutant's helicity. A more stable mutant of domain E was constructed to measure the energy of stabilization contributed by the N-capping box. This study suggests that in stable proteins the N-capping box contributes a part of the energy of conformational stabilization, but in marginally stable proteins this N-terminal motif may be a determining factor of conformational stabilization.

Th-PM-C8

CAN THE EFFECTS OF MUTATIONS ON THE STABILITY OF FIBROUS TWO-STRANDED COILED COILS BE PREDICTED? ((N.J. Greenfield, R.L Hammell, and S.E. Hitchcock-DeGregori)) Dept. Neuroscience and Cell Biology, UMDNJ Robert Wood Johnson Med. Sch., Piscataway, NJ 08854.

Two chain coiled-coil proteins contain two super-coiled right handed α-helices. The sequence is characterized by a heptad repeat, *abcdefg*, in which the *a* and *d* positions are generally hydrophobic and form the interface between the two chains. We have used rat recombinant tropomyosin (TM), as a model, to determine whether the effects of mutations on the stability of two-stranded coiled coils can be predicted by a simple algorithm. We examined the thermal stability of smooth and striated muscle αTM and 7 chimeras in which the 2nd and/or 6th or 9th exons of smooth muscle αTM were replaced with exons from other TMs or with a sequence from the GCN4 leucine zipper. The T_M values of the 9 proteins ranged from 32 to 43 °C. There was a high correlation (P=0.83) of the free energy of folding at 20 °C with the sum of the "hydrophobic moments"[1] of the residues found at the *a* and *d* positions. The stability could also be predicted (P=0.89) by assigning a weight to every amino acid residue in each sequence, depending on its frequency of occurance at the *abcdef* or *g* position in a data base of coiled-coil α-fibrous proteins[2], and summing all the weights. In contrast, there was no correlation of the stability with the helix propensity of their component amino acids as measured by host-guest or Chou-Fasman analyses.
[1]Eisenberg et al. Nature 299: 371-4, 1982. [2]Cohen and Parry, Proteins: Structure Function and Genetics 7: 1-15, 1990. Supported by NIH, AHA-NJ.

Th-PM-C9

DETERMINATIONS OF PROTEIN SECONDARY STRUCTURE USING OPTICAL SPECTROSCOPY--FUNDAMENTAL LIMITATIONS ((Timothy A. Keiderling and Petr Pancoska))
Department of Chemistry, University of Illinois at Chicago, 845 W. Taylor St., Chicago IL 60607-7061

CD, IR, Raman and vibrational CD analyses have limited accuracies for quantitative estimates of average secondary structure. We combined data from far-uv electronic CD with IR vibrational CD of the amide I' and II bands to test the predictability limits. Our methods are based on the principle component method of factor analysis which decomposes the spectra into a sum of independent components. Correlation to structure utilizes the coefficients of the spectral components. Adding coefficients improves the fit of the spectra to structure, but the prediction accuracy of a given technique can be worse for analyses using many spectral components. Adding coefficients from different techniques generally improves prediction for the same number of coefficients. Prediction error is determined from the difference of the computed and crystallographic average secondary structure for one protein left out of a complete series of repeated analyses. From a structural point of view, the results indicate that real spectral information is not being utilized in the projection onto such a simplified picture of the protein structure. A more detailed protein structural descriptor that can better capitalize on the information available from optical spectra leads to a more sequence-specific picture of the protein structure.

Th-PM-C10

LISTENING TO THE HELIX-COIL TRANSITION
((C. Viappiani, J.R. Small, L.J. Libertini and E.W. Small)) University of Parma, 43100 Parma, Italy; Eastern Washington University, Cheney, WA 99004; Quantum Northwest, Inc., Spokane, WA 99207 (viappiani @vaxpr.cineca.it, jsmall@ewu.edu, esmall@ewu.edu)

Photolabile caged proton (2-hydroxyphenyl 2-nitrophenylethyl phosphate, sodium salt) has been used to induce a fast pH jump in aqueous solution containing poly-L-lysine, by pulsing the sample with a nitrogen-pumped dye laser and monitoring with a 1.0-MHz transducer. Time-resolved, volumetric photoacoustic measurements in the temperature range 0 to 35 °C indicate solution volume changes arising from the fast release of protons and from their subsequent binding to the polypeptide. Using a newly-developed experimental protocol, the decay characteristics of the volume changes induced by protonation of the lysine residues have been determined at a variety of pH and ionic strength values. Our data can be modeled as an acid-pulse perturbation of the helix-to-coil equilibrium with transition decay times in the range of 0.5 to 10 μs, depending on the starting pH. Estimates of the accompanying enthalpic change and the molar volume change in the helix-to-coil transition will be presented. Supported by CNR, Italy (CV), GM-51147 and DMI-9362206 (EWS), and GM-41415 (JRS).

Th-PM-D1

SPECIFIC BLOCKING OF THE N-TERMINAL HYDROPHOBIC REGIONS IN cTnC AND CaM INHIBITS ACTIVATION OF MYOFIBRIL ATPase ACTIVITY. ((X. Lin, D.G. Dotson, A. Hudmon, M.N. Waxham and J.A. Putkey)) Departments of Biochem. & Molecular Biology, and Neurobiology and Anatomy, University of Texas Medical School, Houston, TX 77030.

It has been proposed that a critical event in the regulation of striated muscle contraction involves the Ca2+-dependent exposure of a hydrophobic surface in the N-terminal domain of TnC, permitting association with TnI in a manner that is similar to the interaction between CaM and selected targets. To test this hypothesis, CaM and cTnC derivatives were engineered to contain single Cys residues as sites for attachment of specific blocking groups. Cys residues predicted to be on the solvent exposed surface of cTnC (aa 42, 51, 55 and 58) were all highly reactive with DTNB and CPM in the presence or absence of Ca2+, while the reactivity of Cys residues predicted to be in the N-terminal hydrophobic region of cTnC (aa 81 and 45) and CaM (aa 72) were affected by Ca2+. A synthetic peptide, corresponding to the C-terminal 9 aa of the CaM-binding peptide from smooth muscle myosin light chain kinase, was reversibly coupled to selected Cys residues via a disulfide bond. Conjugation of the peptide to Cys 35 or 84 did not inhibit the ability of cTnC to maximally activate myofibril ATPase activity. Conjugation of the peptide to Cys 72 in CaM inhibited its affinity for, and ability to maximally activate CaM-dependent protein kinase. Conjugation of the peptide to Cys 72 in CaM or Cys 81 in cTnC resulted in a reversible, 70% decrease in the ability of these proteins to maximally activate myofibril ATPase activity. Taken together, these results suggest that an accessible N-terminal hydrophobic region in cTnC and is important, but not essential, for activation of myofibril ATPase activity.

Th-PM-D2

MODULATION OF CROSS-BRIDGE KINETICS BY CALCIUM IN RAT MYOCARDIUM. ((T. Wannenburg, G. Heijne, P.P. de Tombe)) The Bowman Gray School of Medicine of Wake Forest University, Winston - Salem, NC 27157.

We studied the effects of calcium on cross-bridge kinetics in rat myocardium to determine whether calcium activates cross-bridges by changes in cross-bridge cycling rates or by a modal "on - off" mechanism. Skinned, isolated, trabecular muscles were studied. The dynamic transfer function of stiffness was measured using sinusoidal sarcomere length perturbations (10 nm) at 18 to 20 perturbation frequencies. The magnitude (panel A) and phase (panel B) of complex stiffness were determined at various calcium concentrations. In the complex plane two exponential processes were resolved as described by Kawai. The characteristic frequencies (*b* and *c*) of these process, averaged over eight muscles are plotted against the developed force in panel C. *b* and *c* have respectively been proposed to reflect cross-bridge attachment and detachment rates. Both *b* and *c* were calcium dependent (panel C) and increased in frequency with increasing calcium concentrations, reaching maximum values of 2 Hz and 14.6 Hz respectively at 1.2 µM calcium, but decreasing again at higher calcium levels. The frequency at which stiffness was at a minimum (dip frequency) similarly reached a maximum at 0.875 µM calcium (panel D) and decreased at higher concentrations. The dip frequency is felt to represent the overall rate of cross-bridge cycling. These data suggest that the regulation of force generation by calcium is mediated in part by changes in cross-bridge kinetics.

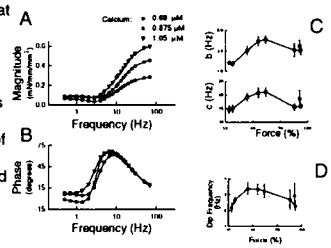

Th-PM-D3

CALCIUM REGULATION OF TENSION REDEVELOPMENT IN SKINNED SKELETAL MUSCLE FIBERS BY CARDIAC TROPONIN C. ((P.B. Chase, D.A. Martyn, C.-K. Wang, B.-S. Pan, R.G. Johnson Jr., M.J. Kushmerick and A.M. Gordon)) Dept. of Radiology, Dept. of Physiology & Biophysics, and Center for Bioengineering, University of Washington, Seattle, WA 98195, and Merck Research Laboratories, West Point, PA 19486.

The rate of isometric force redevelopment (k_{TR}) was measured in Ca^{2+}-activated, skinned fibers from rabbit psoas muscle containing endogenous skeletal troponin C (sTnC) or reconstituted with cardiac troponin C (cTnC) after 90-100% extraction of sTnC. At both maximum and submaximum Ca^{2+}-activation, k_{TR} was characterized during sarcomere length clamp by the monoexponential time constant and the half-time of force recovery after shortening and restretch (Chase *et al.*, 1994, *Biophys J* 67:(Nov)). For TnC reconstitution, purified cTnC from rabbit and cow and recombinant cTnC (over-expressed in *E. coli*) from human (Pan *et al.*, 1994, *Biophys J* 66:A308) and rat were used. Site directed mutants of rat cTnC (C35S, C84S) ensured that results were not due to intramolecular disulfide bond formation, which renders cTnC constitutively activating without Ca^{2+} (Hannon *et al.*, 1993, *Biophys J* 64:1632). Two patterns of k_{TR}-force relations were observed at submaximum Ca^{2+}-activation in TnC reconstituted fibers: (i) little or no difference from sTnC was found for human and bovine cTnC reconstitution, whereas (ii) k_{TR} was significantly elevated for C35S-reconstitution, as was previously found for reconstitution with native, rabbit cTnC (Chase *et al.*, 1994, *Biophys J* 67:(Nov)) or recombinant, human cTnC F77W (Pan *et al.*, 1994, *Biophys J* 66:A308). Thus the properties of TnC modulate k_{TR} at submaximum Ca^{2+}-activation. Support: NIH HL52558, HL51277, AHA WA affiliate and Merck Res. Labs.

Th-PM-D4

THE EFFECT OF CROSSBRIDGES ON THE CALCIUM SENSITIVITY OF THE STRUCTURAL CHANGE OF THE REGULATED THIN FILAMENT. ((K.J.V. Poole, G. Evans*, G. Rosenbaum+, M. Lorenz & K.C. Holmes)) Max Planck Inst. Med. Research, Heidelberg, Germany; * EMBL, DESY, Hamburg, Germany; + Argonne National Laboratory, Chicago, USA.

Previously, we have reported details of the calcium-induced change in the structure of the regulated thin filament as calculated from X-ray diffraction data from skinned, non-overlapped rabbit psoas muscle fibres (Poole et. al. Biophys J. 66, A347, 1994; Holmes;Poole;Lorenz,. Biophys Discussions, Oct 94). The starting model was based on an atomic model of actin-tropomyosin refined against oriented gel data (Lorenz et. al.- J. Mol. Biol, in press). We conclude that when Ca++ binds tropomyosin must undergo an azimuthal rotation of ca. 30° around the filament from an off-state position in which it lies directly over the myosin binding site, to a position in which it would still impinge on the docking of the tip of the upper-50K domain of the myosin head in the actomyosin model of Rayment et. al., Science, 261:58-65,1993. The crossbridge would have to push the tropomyosin a little further round to achieve full docking. These structural findings are entirely consistent with the biochemical data on the regulation of cross-bridge binding which show that all binding is blocked in the Ca++ -free state (at least at physiological ionic strengths), and that Ca++ opens the actin site up for weak binding but that the level of strong binding depends on the head concentration and shows cooperativity (McKillop & Geeves, Biophys. J. 65: 693-701). The titration curve of the the structural change of the thin filament against Ca++ concentration in the absence of cross-bridges shows little cooperativity and has a lower Ca++ sensitivity than force production in these fibres (note error in Poole et al. Biophys J.66, A347, 1994 in which "sharper" should read "less sharp" in the last sentence!). We have performed similar structural titrations in the presence of crossbridges and show that both Ca++ sensitivity and cooperativity are enhanced. Details will be presented.

We thank the Philadelphia Biostructures team at beamline X9B, NSLS, Brookhaven.

Th-PM-D5

CORRELATION OF TROPONIN I FLUORESCENCE WITH FORCE IN SINGLE RABBIT PSOAS FIBERS. ((J.M.Chalovich & B.Brenner)) East Carolina Univ., USA, & Medical School Hannover, FRG.

Activation of skeletal muscle is initiated by an alteration of troponin and tropomyosin on the actin filament. In solution, the state of activation of the actin can be determined by fluorescent probes on either troponin I or tropomyosin. We have applied this technique to skinned rabbit psoas fibers by replacing native TnI with IANBD labeled TnI. This procedure did not appreciably alter the fiber mechanics. The fluorescence was at a maximum in the relaxed state, independent of ionic strength, and at a minimum in the fully Ca^{2+} activated fiber. The Ca^{2+} dependence of fluorescence was seen both in and out of filament overlap. Strong binding cross-bridges produced the same effect as Ca^{2+}: (i) In the presence of PPi, fluorescence was at its minimum, independent of Ca^{2+}. (ii) In the presence of ATPgS, Ca^{2+} was sufficient to produce the maximum fluorescence change although cross-bridges with ATPγS occupy weak binding states. Thus, in contrast to the situation in solution, Ca^{2+} appears to be sufficient for full activation of the thin filaments. Also, weakly bound cross-bridges, which we showed to be necessary for force production, do not appear to interact with the regulated actin filament in the same way as strong binding cross-bridges.
Supported by DFG 849/1-4, NIH, AR40540 and NATO 930448.

Th-PM-D6

EVALUATION OF "STERIC BLOCKING" OF WEAK BINDING CROSS-BRIDGES AT MODERATE IONIC STRENGTH. ((A.M. Resetar, R.H. Hartwell & J.M. Chalovich)) East Carolina University School of Medicine, Greenville, NC 27858-4354, USA.

Upon the addition of Ca^{2+} to vertebrate striated muscle filaments, there is a well described shift of the regulatory protein tropomyosin which appears to be linked to disinhibition of ATPase activity and force production. The question is how this change in the position of tropomyosin on the actin filament alters contractility. Although the movement of tropomysoin leads to a 20-fold change in the affinity of strong binding crossbridges, weak cross-bridge binding is altered only 2 to 5-fold at ionic strengths between 18 and 60 mM. In contrast, the k_{cat} for ATP hydrolysis increases by more than 20-fold upon the addition of Ca^{2+} suggesting that some kinetic aspect of regulation is most important. Recently, it has been suggested that steric blocking of strong binding states such as S1-ADP exists only above 50 mM ionic strength and involves only 66% of the S1-binding sites on actin. We have begun to test whether steric blocking of weak binding crossbridges can be observed under similar conditions.

The kinetics of binding of S1-ADP to regulated actin in the absence of Ca^{2+} was measured over a range of ionic strengths. No lag in S1-ADP binding was observed below 50 mM ionic strength, but the size of the lag attributed to steric blocking did increase with increasing ionic strengths above 50 mM. We then measured the binding of pPDM-S1, an excellent weak binding state model, to actin at ionic strengths greater than 50 mM with high concentrations of pPDM-S1. Our early results show that pPDMS-1 binds to regulated actin even in the absence of Ca^{2+}.

Th-PM-D7

THE MECHANISM OF TROPOMYOSIN REGULATION OF ACTO-S1 ATPase.
((J. Shi, C. Shen, and P. Dreizen)) Physiology & Biophysics, SUNY Brooklyn, Brooklyn, NY 11203.

A molecular mechanics analysis indicates 3 different states for actin-tropomyosin (TM), in which TM rotates clockwise from OFF to NEAR-ON and FAR-ON positions. The actin-TM sites and the main actin-S1 sites in subdomain-1 (Rayment et al, 1993) are separate in all 3 states. OFF-state actin-TM sites involve glu334 and asp25, at base of actin(1-28) loop. Actin(1-5) has been reported to be closely linked to activation of acto-S1 ATPase, but is > 25Å distant from TM. In studies using regulated acto-S1 and EDC, a zero-length cross-linker, we find that formation of acto*HC EDC complex (at/near asp1) is Ca^{2+}-sensitive in presence of ADP or AMP-PNP. Further studies at high pressure confirm that formation of acto*HC EDC complex and acto-S1 ATPase show comparable Ca^{2+}-sensitivity. In studies with glutaraldehyde, the complex between arg28 and HC is also Ca^{2+}-sensitive in presence of ADP. These results suggest a model for Ca^{2+}-regulation in which OFF-state TM abuts upon the base of actin 1-28 loop, inducing a conformational change transmitted from the loop-base to the asp1 region, turning off acto-S1 ATPase. The Ca^{2+}-troponin transition could generate a 90° rotational movement of TM between OFF and NEAR-ON states, but seems unlikely to cause a 180° turn. Some S1 binding sites are near TM residues in OFF and NEAR-ON states, suggesting that S1 interaction is also needed for rotation into FAR-ON state. The present model is consistent with 3 kinetic intermediates (Geeves et al) and EDC studies showing transitions at high and low Ca^{2+}.

Th-PM-D8

STERIC-BLOCKING BY TROPOMYOSIN VISUALIZED IN RELAXED FROG MUSCLE THIN FILAMENTS
((W. Lehman[1], R. Craig[2], and P. Vibert[3])) [1]Dept. Physiology, Boston Univ. Sch. Med., Boston MA 02118; [2]Dept. Cell Biology, Univ. Mass. Med. Sch., Worcester MA 01655; [3]Rosenstiel Ctr., Brandeis Univ., Waltham MA 02254.

Native troponin-regulated frog skeletal muscle thin filaments maintained in EGTA in the "off-state" were examined by negative-staining. 3-dimensional reconstructions revealed typical actin monomers and longitudinally continuous strands of density which followed the innermost edge of the outer domain of successive actin monomers along the surface of the long-pitch actin helices; these strands presumably represent tropomyosin, possibly in combination with troponin-T or other extended parts of the troponin complex. Although this arrangement has long been predicted on the basis of X-ray diffraction data, tropomyosin strands have not previously been seen in the off-state in vertebrate skeletal muscle. Statistical tests show that the location of the strand is significant at greater than the 99.95% confidence level. These results confirm those obtained on thin filaments from *Limulus* (Lehman *et al. Nature 368*, 65:1994) and emphasize the general nature of constraints imposed on tropomyosin by troponin. In fact, the tropomyosin position we observe corresponds well with that derived by Poole *et al.* (1994) who fitted X-ray diffraction data on intact muscle to the atomic model of F-actin. If the position of tropomyosin is stabilized by troponin in relaxed muscle, it would be expected to prevent strong myosin-crossbridge attachment, block crossbridge cycling and thereby cause muscle relaxation.

PHOTOSYNTHESIS—REACTION CENTERS

Th-PM-E1

IS CHLORINE LIGATED TO MN IN THE OXYGEN-EVOLVING COMPLEX IN PHOTOSYSTEM II? RESULTS OF EXAFS STUDIES OF ORIENTED BR-SUBSTITUTED PHOTOSYSTEM II.
((J. Andrews, A. Rompel, R. Cinco, M.J. Latimer, W. Liang, T. Roelofs, V.K. Yachandra, K. Sauer, M.P. Klein))
Structural Biology Division, LBL, & Dept. of Chemistry, UCB, CA 94720.

The evolution of oxygen in photosystem II (PS II) is catalyzed by a cluster of 4 Mn atoms. This Mn cluster cycles through various S-states (S_0 - S_4) as it accumulates the four necessary oxidizing equivalents, releasing O_2 during the S_3 to S_4 transition. Chloride and calcium are essential cofactors for oxygen evolution activity. Cl^- can be replaced with Br^- or I^- with retention of activity. It has been postulated that halide is a ligand to Mn, but the evidence up to the present has not been conclusive.

The structure of the Mn cluster in the oxygen evolving complex (OEC) is being studied by X-ray absorption spectroscopy and we have proposed a structure consisting of two di-μ-oxo bridged Mn binuclear units, linked by mono-μ-oxo and carboxylato moieties. Studies of oriented native and ammonia-treated PS II have yielded highly dichroic K-edge and extended x-ray absorption fine structure (EXAFS) , indicative of an asymmetric tetranuclear cluster. The structure of the Mn complex and the orientation of the complex in the membrane within the context of the x-ray absorption data are discussed. The present studies of oriented PS II in which Br^- has replaced Cl^- in the OEC will be presented, and possible implications for the location of Cl^- in the OEC will be discussed.

Th-PM-E2

OXIDATION STATE CHANGES OF THE MN CLUSTER IN THE FLASH-INDUCED S-STATES OF PHOTOSYSTEM II: DETERMINATION BY X-RAY ABSORPTION SPECTROSCOPY.
((W. Liang, T.A. Roelofs, M.J. Latimer, R. Cinco, A. Rompel, J.C. Andrews, V.K. Yachandra, K. Sauer and M.P. Klein)) Structural Biology Division of LBL and Dept. of Chemistry, UC Berkeley.

The valence state changes of the Mn cluster in the S-states of the oxygen-evolving complex in photosystem II were studied by Mn K-edge spectroscopy. These S-states are prepared at room-temperature by saturating, single-turnover flashes from a Xe-lamp or a Nd-YAG laser. The flash-dependent oscillation in the amplitude of the multiline EPR signal was used to characterize the S-state composition, and further used to construct "pure" S-state Mn K-edge spectra. The edge position (determined by the zero-crossing of the second derivatives) shifted to higher energy by 1.8 eV after the formation of the S_2 state from the S_1 state. We have observed reproducible shift of only ~0.3 eV during the S_2 to S_3 transition. We have also examined the shapes of the second derivatives of the K-edge spectra of these S-states. A feature at ~6553.0 eV disappeared during the $S_1 \rightarrow S_2$ transition. There is no significant difference of the shape between the S_2 and S_3 states. The narrower shape of the second derivative of the S_0 state was distinct from the rest of the S-states. The edge position of the S_0 state was 1.6 eV to lower energy than that of the S_1 state. Both the edge position and the shape of the spectra were suggestive of one Mn(II) in the Mn cluster in the S_0 state. Our results do not agree with those published by Ono and coworkers[1] which reported an $S_2 \rightarrow S_3$ edge shift larger than that for the $S_1 \rightarrow S_2$ transition, and which also precluded the presence of Mn(II) in the S_0 state.

[1]Ono, T.-A., Noguchi, T., Inoue, Y., Kusunoki, M., Matsushita, T. & Oyanagi, H. (1992) *Science 258*, 1335.

Th-PM-E3

DIFFERENCE FTIR STUDY OF THE PHOTOSYNTHETIC WATER OXIDIZING COMPLEX.
((Jacqueline J. Steenhuis and Bridgette A. Barry)) Department of Biochemistry, University of Minnesota, St. Paul, MN 55108.

Water oxidation occurs at the manganese cluster of Photosystem II. Illumination of the water oxidizing complex causes it to cycle through five oxidation states S_n, where n refers to the number of oxidizing equivalents stored. The S_1 state is the dark stable state. The S_4 state is unstable and converts rapidly to S_0 with release of oxygen. When illuminated at 200 K, the S_2 state exhibits a multiline EPR signal centered around g=2 (Dismukes, G.C., & Siderer, Y. (1981) *Proc. Natl. Acad. Sci. U.S.A.* 78, 274-278). Illumination at 130 K generates a derivative shaped EPR signal at g=4.1 (dePaula, J.C., Innes, J.B., & Brudvig, G.W. (1985) *Biochemistry* 24, 8114-8120). Both EPR signals have been attributed to the manganese cluster in the S_2 state. We have obtained the difference FTIR spectra associated with the S_1 to S_2 transition in spinach photosystem II at 130 and 200 K. In the spectral region from 1900-1200 cm^{-1} differences in these data can be observed. These spectral differences could be due to structural changes in the protein environment of the manganese cluster. These data have been compared to the spectrum associated with chlorophyll oxidation and quinone reduction at 80 K. We have also obtained difference FTIR spectra of the S_1 to S_2 transition in cyanobacterial photosystem II at 200 K. These spectra are similar to those obtained on spinach photosystem II at the same temperature. We are now able to use isotopic labelling and site directed mutants to identify the structural changes associated with the S_1 to S_2 transition.

Th-PM-E4

PHOTOPROTECTION IN PHOTOSYSTEM II: THE ROLE OF CYTOCHROME b559.
((M. Poulson[1], G. Samson[2], and J. Whitmarsh[1,2])) [1]Dept. of Plant Biology, Univ. of Illinois, Urbana IL. 61801, [2]Photosynthesis Research Unit, Agricultural Research Service/USDA, Urbana, IL 61801

Photosystem II reaction centers in plants, algae and cyanobacteria are susceptible to damage by excess light that irreversibly impairs activity and eventually results in proteolytic degradation of at least one of the core proteins. The sequence of events and underlying molecular mechanisms that lead to photoinhibition are poorly understood. We have shown that damage to PSII caused by excess light is strongly dependent on the redox state of a one-electron component (Nedbal et al. 1992 Proc. Natl. Acad. Sci. 89:7929-7933). The irradiation-induced loss of the oxygen evolving capacity of PSII in isolated thylakoid membranes is slow when the redox component is oxidized and increases by more than 15-fold when it is reduced. Anaerobic potentiometric titrations of the rate of photoinhibition indicate a redox component with a nearly pH -independent midpoint potential of 20-30 mV in thylakoid membranes. We suggest that the low potential form of Cytochrome b559 (Cyt b559LP) is a likely candidate for redox control of the rate of photoinhibition. In isolated thylakoid and PSII enriched membranes under anaerobic conditions, we observe that light induces the photoreduction of approximately 80% of Cyt b559LP. In thylakoid membranes, the time course of this reduction precedes both the variable fluorescence quenching and loss of water oxidation that are associated with photoinhibition. The results can be explained in terms of a protective PSII electron transport pathway that requires a one-electron redox component to be in the oxidized state to function.

Th-PM-E5

ULTRAFAST LOSS CHANNEL COMPETING WITH EXCITATION ENERGY TRANSFER FROM THE ACCESSORY BACTERIOCHLOROPHYLL IN PHOTOSYNTHETIC RCs. G.Hartwich, M.Friese, A.Ogrodnik, H.Scheer* and M.E.Michel-Beyerle, Inst. f. Phys. und Theor. Chemie, TU München, 85748 Garching and *Botanisches Institut, Universität München, 80638 München, FRG.

Excitation energy transfer (EET) between the cofactors of reaction centers (RCs) of *Rb. sphaeroides* is known to occur within 100fs[1]. The efficiency of the EET $\Phi EET(\lambda)$ of a pigment absorbing at wavelength λ to $^1P^*$ can be investigated by comparing the excitation spectra of the $^1P^*$ fluorescence $F(\lambda)$ with the absorption spectra $OD(\lambda)$ according to: $F(\lambda) \propto \lambda/hc \cdot \Phi EET(\lambda) \cdot \Phi F \cdot (1-10^{-OD(\lambda)})$ (ΦF=fluorescence quantum yield of $^1P^*$ after direct excitation at 860nm). In native RCs a depression of the 800nm band in the fluorescence excitation spectrum was found indicating $\Phi_{EET \simeq 90\%}$ for the accessory bacteriochlorophylls (B). In order to compete sufficiently with EET the process responsible for this loss must occur in $\simeq$ 1ps. Only electron transfer is likely to be fast enough. Electric field effects of $F(\lambda)$ strongly depending on λ corroborate this notion. The reactions $^1B^* \rightarrow B^+H^- \rightarrow P^+H^-$ [2] or $^1B^* \rightarrow P^+B^- \rightarrow P^+H^-$ are possible candidates. In RCs with B having been chemically exchanged against 13^2-OH-Ni-BChl$_a$ [3] (Ni-RCs) ΦEET<40% throughout the spectrum except in the Q_x band of P around 600-650nm. This high loss is due to ultrafast internal conversion and intersystem crossing in the Ni-Bchl, which together must be faster than 70fs. In this case the loss mechanism is not expected to be electric field dependent. Indeed, the electric field effects on ΦEET were found to be neglegible. [1] J.Breton et al. PNAS USA, 83 (1986) 5121-5125. [2]S.Fischer, P.O.J.Scherer, Chem. Phys. 115 (1987) 151-158. [3] G.Hartwich, Thesis (1994) Munich.

Th-PM-E6

NO CHANGE OF PRIMARY CHARGE SEPARATION RATE ON LOWERING THE ENERGY OF P^+B^- BY EXCHANGING 13^2-OH-Ni-BChl$_a$ FOR THE ACCESSORY BChl$_a$. M.Friese, G.Hartwich, A.Ogrodnik, H.Scheer* and M.E.Michel-Beyerle, Inst.f.Phys.u.Theor.Chemie, TU München, 85748 Garching and *Botanisches Inst., Universität München, 80638 München, FRG.

The accessory bacteriochlorophylls (BChl) in reaction centers (RCs) of *Rb. sphaeroides* R26 have been replaced by 13^2-OH-Ni-BChl$_a$ [1] (Ni-RCs). Compared to Mg-Bchl the *in vitro* redoxpotential of Ni-BChl^-_a is by 300mV more positive. In Ni-RCs recombination dynamics[2] of $P^+H_A^-$ locate the energy of $P^+B_A^-$ $\simeq$200meV below $^1P^*$, entailing charge separation (CS) to $P^+B_A^-$. The analogous energy gap in native RCs is $\lesssim$60meV[3] allowing for both, electron transfer (ET) to P^+B^- and superexchange mediated ET to P^+H^-. Since CS is activationless, lowering the energy of P^+B^- as in Ni-RCs should slightly reduce its rate if ET to P^+B^- prevails. In case of superexchange CS in native RCs, this would eventually lead to direct population of $P^+B_A^-$ and an increase of the CS rate. Time-resolved fluorescence measurements of Ni-RCs and native RCs show: (1) The average lifetime of the fluorescence emitted within the instrumental response-time (50ps) increases from 3.2ps[4] to $\simeq$9.5ps at 280K being slightly activated. Thus, direct ET to P^+B^- is proven for both RCs, with the Ni-RCs being in the inverted region. (2) In Ni-RCs fluorescence components with lifetimes in the range 200ps-3ns are vastly reduced as compared to native RCs, where these components were attributed[5] to a minority (<2%) of RCs undergoing slow superexchange CS due to energetic inhomogeneity of P^+B^-. In Ni-RCs the energetic dispersion does not induce significant slowing of CS due to activation or switching to a superexchange mechanism, because $P^+B_A^-$ is deep enough in the inverted region. [1]G. Hartwich, Thesis (1994) TU München [2] M.E. Michel-Beyerle et al., to be published. [3]A.Ogrodnik, BBA 1020 (1990) 65. [4]P.Hamm et al. BBA 1142 (1993) 99. [5]A.Ogrodnik et al. J. Phys. Chem. 98 (1994) 3432.

Th-PM-E7

SINGLE CRYSTAL HIGH-FIELD EPR ON THE PRIMARY ELECTRON DONOR OF A REACTION CENTER HETERODIMER MUTANT.

((M. Huber[#,#], J.T. Törring°, C.C. Schenck[&], K. Möbius°)) [#]Institute of Organic Chemistry, FU Berlin, Takustr. 3, 14195 Berlin, FRG; °Institute of Experimental Physics, FU Berlin; [&]Department of Biochemistry, Colorado State University, Ft. Collins, CO 80523.

High-field/high-frequency EPR at 95 GHz has been used to investigate the electronic structure of the primary electron donor (D, a special pair of bacteriochlorophyll (BChl) molecules) in reaction centers from *Rhodobacter sphaeroides*. In particular, we have measured the anisotropy of the G-tensor ($\underline{G}$) of the cation radical of D (D^+). The G-anisotropy of D^+ is small, requiring EPR at high frequencies to obtain sufficient spectral resolution. $\underline{G}$ contains information on the overall symmetry of the electronic structure and on excited state properties of the radical. For D^+ in wild type reaction centers, where the unpaired electron is delocalized over the two BChls, the principal directions of the G-tensor are known [1] and are largely consistent with the dimeric nature of D. In heterodimer mutants, one BChl of D is replaced by a bacteriopheophytin. The resulting asymmetry causes the unpaired electron to be localized on the BChl [2]. Consequently, G properties of this mutant should give insight into the G-tensor of the monomeric system, as a reference for the interpretation of the dimer. Single crystal high-field EPR on D^+ in the HL(M202) heterodimer mutant reveals that, in contrast to planar π-electron systems, the direction of the smallest G-tensor component deviates from the normal of the plane of the π-electron system. The axes of $\underline{G}$ in the heterodimer are close to those of the native system. This suggests that D_L, the BChl in HL(M202), makes a strong contribution to the G-tensor of the dimer. [1]R. Klette et al., *J. Phys. Chem.* 97, 2015 (1993); A. van der Est et al., to be published; [2] M. Huber et al. in: Reaction Centers of Photosynthetic Bacteria, M.-E. Michel-Beyerle (ed.), Springer Verlag, Berlin (1990) p. 219ff

Th-PM-E8

INFLUENCE OF HYDROGEN BONDS TO $P^{+\cdot}$ IN MUTANT REACTION CENTERS OF *RB. SPHAEROIDES* STUDIED BY ENDOR AND TRIPLE RESONANCE *

((J. Rautter, F. Lendzian, C. Schulz, M. Kuhn, W. Lubitz)), Max-Volmer-Institut, TU Berlin, D-10623 Berlin, Germany; ((X. Lin, J. C. Williams, J. P. Allen)), Chemistry Dept., Arizona State University, Tempe AZ 85287-1064, USA

The hyperfine structure of $P^{+\cdot}$ (a BChl *a* dimer) was determined in RCs of 12 mutants from *Rb. sphaeroides* with different hydrogen bonding patterns between the conjugated carbonyl groups of P and histidine residues of the protein. Depending on the positions of the H-bonds different spin densities are obtained with the extremes of a localization on either half of the dimer, P_L or P_M. These effects are attributed to the influence of the H-bonds on the orbital energies of the two BChl *a* halves of the dimer. These data are correlated with electron transfer rates involving $P^{+\cdot}$, i.e. the reduction by cytochrome c_2 and the charge recombination from Q_A^-. In addition the influence of H-bonds on the mutant HL(M202), that has a BChl-BPhe heterodimer as the primary donor, is reported.

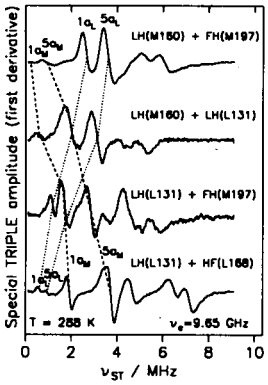

Fig.: S-TRIPLE of 4 mutants, CH_3 lines (pos. 1a, 5a) for P_L and P_M are indicated.

* supported by DFG, NIH, NSF, and NATO

Th-PM-E9

INTEREXCITON STATE RELAXATION IN ALLOPHYCOCYANIN.

((Maurice D. Edington, Ruth E. Riter, William J. Doria, and Warren F. Beck)) Department of Chemistry, Vanderbilt University, Nashville, TN 37235.

We have performed femtosecond transient absorption and dichroism studies on allophycocyanin, a linear tetrapyrrole-containing light-harvesting protein located in the core of the phycobilisome of cyanobacteria. We are examining the role in photosynthetic excitation transfer of the probable C_3 array of tetrapyrrole dimers formed in allophycocyanin's $(\alpha\beta)_3$ aggregation state. The time-resolved photobleaching/stimulated emission (PB/SE) spectrum of allophycocyanin exhibits a single peak in the 650–660 nm region. Time-resolved spectra obtained with 30 fs or 80 fs excitation pulses exhibit very little PB/SE in the spectral region excited directly by the pump pulse (620 nm), even at the earliest probe delay times following temporal separation of the pump and probe pulses. Calculated pump-probe difference spectra indicate that the time-resolved spectra are best explained by the presence of an ultrafast interexciton level scattering process, which shifts population between the two exciton states expected in a chromophore dimer. The initial relaxation of the optically prepared upper exciton state occurs on a time scale comparable to the pump-pulse duration (< 30 fs). Slower spectral evolution follows this initial relaxation, with time constants detected in single-wavelength transients on the 300 fs–1 ps time scale. These slower processes are assigned to contributions from vibrational relaxation, transient solvation, and exciton localization. Optically heterodyne-detected (OHD) dichroism transients indicate an ultrafast nonexponential relaxation of the initially photoselected transition moment.